

Microarray Profiling in Fibrogenesis Imperfecta Ossium

Vandana Dhiman

Post Graduate Institute of Medical Education and Research

Samarth Saini

University of Minnesota

Sanjay Bhadada (✉ bhadadask@rediffmail.com)

Post Graduate Institute of Medical Education and Research

Manoj Bhasin

Emory School of Medicine Atlanta

Sudhaker Rao

Henry Ford Health System

Research Article

Keywords: Fibrogenesis Imperfecta Ossium, Microarray, Osteomalacia

Posted Date: January 7th, 2021

DOI: <https://doi.org/10.21203/rs.3.rs-138783/v1>

License:  This work is licensed under a Creative Commons Attribution 4.0 International License.

[Read Full License](#)

1 Microarray Profiling in Fibrogenesis 2 Imperfecta Ossium 3

4 Vandana Dhiman¹, Samarth Saini², Sanjay Kumar Bhadada¹, Manoj K. Bhasin³, Sudhaker D.
5 Rao⁴,

6 ¹Department of Endocrinology, Postgraduate Institute of Medical Education and Research,
7 Chandigarh, India; ² Department of Neuroscience ,University of Minnesota, Minnesota,USA; ³
8 Emory School of Medicine, Atlanta, USA, ;⁴Bone & Mineral Research Laboratory, Henry Ford
9 Health System, Detroit, Michigan, USA

10 **Abbreviated title:** Microarray of FIO

11 **Keywords:** Fibrogenesis Imperfecta Ossium, Microarray, Osteomalacia

12 **Type of Article:** Original Article

13 **Word Counts:** Abstract: 110; Manuscript Text: 3552

14 **Corresponding Address for correspondence:**

15 **1 Dr. Sanjay Kumar Bhadada**

16 Professor of Endocrinology

17 PGIMER, Chandigarh, India

18 E-mail: bhadadask@rediffmail.com

19 Phone: +919876602448

20 **2 Manoj K. Bhasin, Ph.D.**

21 Associate Professor Of Biomedical Informatics,

22 Emory School of Medicine, Atlanta, GA 30322

23 Phone: 404-712-9849

24 E-mail: manoj.bhasin@emory.edu

25

26 **Abstract**

27 Fibrogenesis imperfecta ossium (FIO) is a rare, metabolic bone disease clinically characterized
28 by generalized bone pain and fragility fractures in both the axial and appendicular skeleton. The
29 etiology of the disease is unknown and the pathogenesis is poorly understood. In this disorder,
30 collagen arrangement in the bone is disorganized , and causes abnormalities in the organic bone
31 matrix. Genetic cues causing this defect in collagen arrangement are largely undetermined.
32 Microarray analysis showed remarkable changes in gene expression , when we compared gene
33 expression of FIO with the control. Differential gene expression analysis revealed 50 gene
34 signatures, which can be used to organize novel ways to diagnose and treat FIO patients.

35 **Introduction**

36 Fibrogenesis Imperfecta Ossium is a progressively crippling skeletal disorder that is adult-onset
37 and usually fatal. Only 29 total cases of FIO have been reported since it was first described in
38 1950 by Baker and Turnbull¹. It's etiology is unknown but presumed to be genetic, as there have
39 been multiple reported cases of FIO presenting itself in siblings as well as parents and their
40 children. FIO manifests as generalized bone pain and fragility fractures, which can eventually
41 cause skeletal deformities. These bone fractures happen under minimal stress or very minor
42 traumas , and usually occur in weight-bearing and tendon insertion sites. It should be noted that
43 the features of FIO are present everywhere except the skull and the teeth. Ultimately, those
44 affected by FIO become incapable of doing daily activity of life, unable to stand, and are
45 bedridden.

46 The pathogenesis of FIO is mostly understood, and can be pinpointed to the arrangement of
47 collagen fibers. The primary abnormality in FIO is impaired bone mineralization due to defects
48 in collagen arrangement. Bone is a dynamic connective tissue, this dynamicity is maintained by

49 osteoblast and osteoclast cells. Osteoblasts are in charge of laying down the collagen fibers in the
50 bone matrix, but it is osteocalcin (OCN), osteonectin (ON) and osteopontin (OPN) that
51 determine how the fibers are arranged. Currently, it cannot be said if this defect is caused by
52 impaired osteoblasts or abnormalities in OCN, ON or OPN. Many diseases are similarly affected
53 by impaired function of these cell types, such as osteogenesis imperfecta, osteopetrosis,
54 osteoporosis, Paget's disease, fibrous dysplasia, osteomalacia and many more. The key
55 difference between FIO and other osteomalacic conditions is the lack of the birefringence
56 characteristic of normal, oriented collagen fibers. Transmission electron microscopy shows that
57 bones of FIO patients are made up of abnormal collagen fibrils that are often curved and of
58 variable size⁴¹. It is likely this function that enables fractures to occur in even minor trauma and
59 weight bearing conditions.

60 The paucity of literature about the disease and low index of suspicion can also make difficult
61 obtaining an accurate diagnosis. FIO is often misdiagnosed as osteomalacia or Paget's disease
62 because the symptoms of the diseases are very similar, and all three occur in conjunction with
63 increased levels of alkaline phosphate⁴². Usually, diagnosis is confirmed after a bone biopsy
64 shows the reduced birefringence in the collagen fibers. Treatment for FIO is largely ineffective
65 and a complete cure has not been found, mainly due to the scarcity of patients available for
66 randomized trials. Since bone mineralization is defective, treatment usually includes vitamin D,
67 metabolites, calcitonin, bisphosphonates, and corticosteroids, usually to little degrees of success.
68 Recently, growth hormone (GH) has been found to be more effective in treating two brothers
69 with FIO⁴³⁻⁴⁵. They have shown improvements in osteoid thickness and normalization of
70 collagen arrangement, but long term benefits have yet to be determined.

71 The primary objective of this research is to fill in the lack of information about FIO gene data in
72 the current time. Microarray data from this study identifies differentially expressed genes
73 between FIO patients and healthy humans. Finding and indexing these genes may open the door
74 to development of more effective novel therapies for FIO. In addition, this study may also
75 provide insight into the importance of gene regulation in collagen, which is the main organic
76 component of bone matrix responsible for skeletal integrity.

77 **Materials and Methods:**

78 **Patients.** *Ethics statement.* The research design was approved by the Institutional Ethics
79 committee, Postgraduate Institute of Medical Education and Research (PGIMER), Chandigarh
80 India. Informed consent was obtained from all study participants. The study was carried out in
81 accordance with the approved guidelines.

82 *Patients and Clinical sample collection* FIO patient were enrolled in this study. The diagnosis of
83 FIO was established with the help of clinical feature, supported by radiological (Looser's zone)
84 and Tc ⁹⁹ MDP bone scan (super scan with absence of uptake in skull also called 'beheaded
85 scan') and osteomalacia was confirmed by bone histomorphometry (thickened osteoid seam)
86 with loss of birefringence on polarized light microscopy. Total RNA was isolated from Trans-
87 Iliac Bone biopsy (Control Individual (n=1) & Patient (n=1)) using TRIZOL method and global
88 microarray was performed on Affymetrix Genechip HumanPrimview platform and sample
89 descriptions are provided in Table 1(a). The array was performed on duplicate.

90 **Datasets**

91 This study uses data from three datasets: GSE43861, GSE58474, and GSE30159. The primary
92 dataset, GSE43861, contains data from a study conducted by department of Endocrinology
93 comparing two FIO patients and two control samples. GSE58474 contains data comparing

94 mandibular and iliac bone derived cells. Both GSE58474 and GSE30159 were taken from the
95 Gene Expression Omnibus (GEO) database and are used for co-expression network building.
96 The workflow for the bioinformatics analysis in this paper is illustrated in (Figure 1).

97 **Data Quality Control Analysis**

98 A PCA (Principal Component Analysis) was performed on GSE43861 to reduce dimensionality
99 and bring out patterns in the dataset as shown in (Figure 2). PCA was also done on the publicly
100 available datasets GSE72490, GSE30159, and GSE 58474 for dimensionality reduction and
101 quality control of samples within the study. If the quality of the sample is not suitable for the
102 study based on the distribution of PC (Principal Component), it was excluded from the
103 subsequent analysis. Details of each microarray study, including sample descriptions are
104 provided in (Table 2).

105 **Batch Effect Adjustment**

106 The primary goal of this study is to identify differentially expressed genes between normal
107 control and FIO patients. However, data integration to increase the sample size by including the
108 other bone related studies was hindered by batch effects. The pre-processed and normalized
109 datasets were further subjected to ComBat in order to mitigate the batch effects and other
110 undesired variation. To compare the sample clustering patterns, the results were visually
111 examined using the principal component analysis (PCA). Multidimensional scaling of the
112 datasets revealed that before application of the batch adjustment algorithm, each dataset clearly
113 separated from all the others (“batch effect”), whereas when batch adjustment was applied,
114 samples from each dataset were well intermixed.

115 **Identification and Selection of Eligible Gene Expression Datasets for Meta-Analysis**

116 The selection method of an eligible gene signature for FIO is also shown above in (Figure 2).
117 After the microarray analysis of GSE43861 and two other publicly available datasets
118 (GSE30159, GSE 58474), a co-expression network was built by utilizing a WGCNA package.
119 Only interactions with a p-value < 0.05 were included into the expression network. Next, a
120 clustering method was applied to the co expression network in order to identify the subnetwork
121 with maximum connectivity. Cytoscape 3.0.1 was used as the platform for network analysis.
122 The cluster was analyzed with the cytoscape package j Active Modules, which finds
123 subnetworks based on expression activated subnetworks. jActiveModules also provides a
124 ranking co-efficient for each subnetwork. The subnetwork (cluster) with the highest co-efficient
125 was used for our biomarker selection. Subsequently, the CytoNCA cytoscape tool was
126 employed to rank the genes within the selected subnetwork and the genes were ranked based on
127 degree, from highest to lowest.

128 **Microarray Meta-Analysis**

129 To identify the Differentially Expressed Genes (DEGs), GEO2R was used to download the data
130 and group the samples. Once samples are grouped and normalized, expression values were used
131 for the identification of DEGs with the limma package of R based on the thresholds of fold
132 change >2 or <0.5 and FDR adjusted p-value < 0.05. The heatmap of clustering genes were
133 obtained using the heatmap 2 R function.

134 **Functional Gene Set Enrichment Analysis of Shared Differentially Expressed Genes** 135 **(DEGs)**

136 For the exploration of processes involved in the development of FIO, a functional enrichment
137 analysis was also conducted for DEGs after clustering through ShinyGO v0.51 with the

138 thresholds of p-value < 0.05. To obtain the heatmap enrichment terms and genes, GenCLiP2 was
139 applied.

140 **Results**

141 **Microarray data analysis**

142 During the differential gene expression analysis, 6133 out of the 30,218 genes were shown to
143 have statistically significant (adj. P-value cutoff < 0.05) differential expression, whereas 2220
144 genes out of the 35,307 genes show statistically significant (adj. P-value cutoff < 0.05)
145 differential expression. To obtain a substantial gene list for analysis, the differentially expressed
146 genes were further filtered by taking a fold change ≥ 1.5 . Only 325 genes were expressed with a
147 fold change ≥ 1.5 (311 down-regulated and 14 up-regulated genes; Table 1 (b and c). The gene
148 list related to growth hormones was also extracted, as shown in Table 1(d). To facilitate the co-
149 expression network, we also used other publicly available datasets related to bone disease
150 GSE58474 and GSE30159. All the raw and normalized data were deposited at NCBI's Gene
151 Expression Omnibus and are accessible through GEO Series accession number: GSE43861
152 (<http://www.ncbi.nlm.nih.gov/geo/query/acc.cgi?Acc=GSE43861>.)

153 **Co-expression Network analysis**

154 To facilitate the list of genes, we built a co-expression network by using only the expression
155 matrix from GSE43861. However, the co-expression network retrieved through this dataset
156 yielded a disjoint network. Therefore, we pooled the expression matrix from GSE43861 with
157 other publicly available datasets as shown in GSE58474 and GSE30159. These datasets contain
158 information from studies with similar skeletal diseases. The gene list from Table 1 (b and c)
159 which shows differentially expressed genes had 266 overlapping genes out of 325 from

160 GSE43861. Then, we built a co-expression network with p-value 0.05 for each interaction as
161 shown in (Figure 3).

162 In order to rank the 248 genes based on their connectivity with co-expressed genes, we
163 calculated centrality measures for the network (Figure 3). The outcome of the centrality measure
164 is shown in (Table S1), where the genes are ranked based on degree of centrality. Furthermore,
165 we applied the clustering method on the network as shown in (Figure 3A) in order to reduce the
166 dimensionality of network. Then, we used jActiveModules, a clustering method which clusters
167 the nodes based on the significance in expression levels. After clustering, we selected the cluster
168 with maximum connectivity score as shown in (Figure3B &Table3) and (Figure3C). The
169 maximum connectivity score in (Figure3C) is 7.159 as compared to another larger cluster
170 Module_0_3 shown in (Figure S3C).

171 Thus, 50 genes were selected to be studied based on the clustering analysis. The ranked list of 50
172 genes can be seen in (Table 4). In this table, genes are ranked based on the degree of connectivity
173 (Figure3C). Figure 4 shows the heatmap of the 50 genes in our study from GSE43861. The
174 control samples are grouped as green and FIO patient samples are grouped as blue.

175 **Gene Set Enrichment Analysis for Identification of Biological Pathways Gene Ontology** 176 **Terms**

177 To identify the overrepresented biological pathways and gene ontology terms associated with the
178 50 differentially expressed genes, we performed gene set enrichment analysis using the Shiny Go
179 v0.50 tool by inputting the list of 50 DEGs. The outcome of this analysis is shown in (TableS2).
180 Gene ontology terms and biological pathways were considered significantly overrepresented if
181 they showed an adjusted p-value <0.05 for GO (BP, CC, MP), Reactome, KEGG, or MSigDB.

182 The results from (Table S2) and (Figure 5) shows that the top enriched pathways are in BP
183 (Biological Process): “Cellular catabolic process ”,“Catabolic process ”,“Negative regulation of
184 metabolic process ”,“Macromolecule catabolic process ”, and “Cellular macromolecule catabolic
185 process” where enriched genes are more than 15 out of 50 genes. For the cellular component:
186 “Non-membrane-bounded organelle ”,“Intracellular non-membrane-bounded organelle
187 ”,“Vesicle ”,“Cytoskeleton ”,“Extracellular organelle ”,“Extracellular exosome ”, and
188 “Extracellular vesicle” where the minimum enriched genes are 12. For MP (molecular process):
189 “Nucleic acid binding ”,“Metal ion binding ”,“RNAbinding ”, and “Structural molecule activity”
190 are the top enriched terms with minimum genes greater than 9. Pathways from Reactome and
191 MSigDB (curated) are “Reactome: R-HSA-168256 Immune System”,“Reactome:R-HSA-162582
192 Signal Transduction”,“Reactome:R-HSA-392499 Metabolism of proteins”,“Reactome:R-HSA-
193 168256 Immune System”,“Reactome:R-HSA-162582 Signal Transduction”, and “Reactome:R-
194 HSA-392499 Metabolism of proteins” for mapped genes more than 10 for each pathways out of
195 the 50 genes. We also looked into Hallmark MSigDB and KEGG and obtained “MSigDB :
196 Hallmark MYC Targets v1”,“ MSigDB: Hallmark Reactive Oxygen Species Pathway”, “
197 MSigDB: Hallmark epithelial mesenchymal transition”, “Carbon metabolism”, “Ribosome”,
198 “Autophagy”, “RNA transport”, “Regulation of actin cytoskeleton”, “Huntington disease”,
199 “Bacterial invasion of epithelial cells”, and “Fc gamma R-mediated phagocytosis” pathways
200 where a minimum of 2 genes are mapped. The function of each gene is using Gene Clip 2.0.
201 However, 5 genes—ATP5G2, MRPL23, SPOP, POLR2L, and SAP30BP—did not map to any
202 functions.

203 **Discussion**

204 The current study centers around two patients of ages 35 and 40 who are currently living with
205 FIO. We carried out a microarray study on the mRNA extracted from patients. Differential
206 expression analysis and other network biology methods were employed to establish 50
207 differentially expressed gene signatures. Our results show a significant number of differentially
208 expressed genes in the patient cells. The list of genes including rankings is available in (Table 4)
209 along with (Table S2) and the most significant an Ingenuity Pathway Analysis (IPA) network
210 diagram Figure 5a. The red circles in (Figure 5a) shows the down regulated genes whereas the
211 blue shows up regulated genes. The retrieved genes, such as ATG4B, ATG3 [Table S2: KEGG],
212 are associated with autophagy. Autophagy is closely associated with processes such as cellular
213 catabolic and metabolic processes³. In our enrichment from (Table S2: GO BP), the enriched
214 genes and biological processes are also associated with catabolic processes. There are about 15
215 genes (PGK1, FBXL5, SPOP, CAT, ATG3, PRDX2, ATG4B, DDX5, TCIRG1, CSDE1, VIM,
216 EIF4G1, CLTA, RPS23, RPS9) that are associated with cellular catabolic processes. With this in
217 mind, it has been studied in previous works that autophagy have a known role in multiple
218 osteoblast functions⁴. In the current approach, due to the autophagy in macromolecules and
219 organelles also reported in our results (Table S2: GO CC, Non-membrane-bounded organelle and
220 Intracellular non-membrane-bounded organelle-23 genes: RPS23, RPS9, MRPL28, YY1, TPM4,
221 POLR2L, MRPL23, AIF1, VIM, LIMCH1, DDX5, GNAI2, SAP30BP, CCDC85B, MYL12A,
222 COTL1, CLTA, FGD3, TIAL1, WASF2, SF1, EIF4G1, LRRFIP1), these genes are degraded and
223 have demonstrated their crucial role in bone and muscle cell homeostasis. Any kind of
224 abnormality in autophagy leads to osteoporosis and sarcopenia³. Furthermore, the genes from
225 (Table S2: GO MP Metal ion binding: SPARC, POLR2L, AIF1, FBXL5, EGR1, LIMCH1,
226 RSBN1, YY1, MYL12A, PHC1, GNAI2, CAT, EIF2S2, FGD3, TPM4, SF1, SDHD) control

227 metal ions that play several major roles in proteins such as structural, regulatory, and enzymatic.
228 For instance, the gene SPARC relates to osteonectin (ON), which is secreted from osteoblasts
229 and bind calcium. More examples include AIF1, a calcium binding gene associated with synovial
230 fluid (SF) derived from patients with either RA or osteoarthritis(OA) ⁵. AIF1 is also reported to
231 have a role in bone destruction as well as synovitis⁵ In addition, the gene FBXL5 limits oxidative
232 stress maintained in hematopoietic stem cells ⁶, the CAT gene variants are known to have a role
233 in acatalasemia, and POLR2L, EGR1,YY1, and SF1 are all zinc binding genes. The results
234 clearly show that the 50genes retrieved by our disease (FIO) have role in bone deformity and
235 Ca+, Zn+, and metal ion enrichment. The overview in terms of gene functions of 45 of the 50
236 genes is shown in Figure 5(b). As per (Table 4), DDX5 is a top ranked gene on the list based on
237 higher degree. DDX5 is upregulated in FIO patients and has a distinct association with Myotonic
238 Dystrophy (C0027126: Myotonic Dystrophy, DisGeNET Curated, P-value: 8.02E-03). Myotonic
239 Dystrophy is associated with increased risk of bone fragility and progressive muscle weakness
240 on bone strength⁷. Similarly, the SPOP gene, known as a POZ domain gene is a regulator of
241 skeletal development, and may lead to shorter digit bones and lower bone density⁸. SDHD has an
242 association with abnormality of limb bone (HP:0040068 (HPO_PHENOTYPE_GENE)),
243 SAP30BP ⁹, and EIF2S2, EIF4G1,and EIF4A2 all belong to a eukaryotic translation initiation
244 factor gene family that are known to have role in apoptosis in osteosarcoma cells. Osteosarcoma
245 is a type of cancer that produces immature and weak bones¹⁰. Similarly, the SRSF3 and FBXL5
246 genes are also associated with osteosarcoma, leading to under developed bones^{20,21}. The CAT
247 gene is related to catalase activities, and has a defined role in bone mineral density ¹¹. LRRFIP1
248 is a repressor gene and when it bounds with non-coding RNAs of TNF genes, it acts as
249 stimulator in bone resorption.¹² COX2 is also known as Cyclo-Oxygenase 2, and is an essential

250 marker for bone fracture healing when upregulated, which is analogous to the case for our FIO
251 patients¹³. WASF2 expression is related to bone formation in animals and humans with
252 intermittent PTH administration via the WNT and phosphoinositide-dependent protein kinase
253 signaling pathways¹⁴. YY1 is accurately known to have functions as growth factors and could
254 generate bone morphogenetic protein (BMP) in synergy with SMAD1 and SMAD2 genes¹⁵.
255 FAM134C is known to have associated with distal sensory loss in lower limbs¹⁶. In our FIO
256 patients, TPM4 is down regulated and it has known effects on bone formation, for example,
257 upregulation of TPM4 has already been reported to have higher expression of untreated
258 osteoblasts¹⁷. Radial spoke proteins RSP23 and RSP9 are associated with controlling dynein
259 (family of cytoskeletal motor proteins) activity and flagellar motility¹⁸, which might disturb
260 motor-specific functions in osteoclast formation and bone resorption¹⁹. The RSBN1 gene is
261 downregulated in patients known to have marginal association in juvenile idiopathic arthritis
262 (JIA)²². TMEM123 has been reported to have role in oncosis, a condition refers to have series of
263 cellular reactions following injury that precedes cell death^{23,24}. TIAL1 and POLR2L are genes
264 that are enriched with “Reactome:R-HSA-6803529 FGFR2 alternative splicing” as shown in
265 (Table S2: REACTOME), which was previously reported to have role in bone formation²⁵.
266 SEC63 as shown in (Table S2: GO-MF) is enriched with metal ion binding. Metal ion binding is
267 associated with bone health through various metal metabolisms. The ATG4B, ATG3, and
268 CSDE1 genes have not been reported for any bone related diseases, however, as shown in (Table
269 S2: GO-KEGG), these genes are enriched with autophagy and multiple studies have proved the
270 role of autophagy in bone deformity as discussed earlier in this section. CSDE1, ATP5MC2
271 (ATP5G2) and PRDX2 are all enriched in “negative regulation of lipid localization” which is
272 associated with energy metabolism²⁶ as shown in Figure 5(b). SF1, SRSF3, POLR2L, DDX5 as

273 shown in Figure 5(b) enriched through “Formation of the Spliceosomal E complex”.The
274 spliceosome is an essential step in gene expression where it combines snRNAs and it removes
275 introns from transcribed pre-mRNA. While that may be true, the role of these spliceosomal genes
276 are poorly studied. However, the presence of a few spliceosomes indicates its position in
277 autosomal recessive developmental defects²⁷. The CHID1, CLTA, TCIRG1, VIM, FCGR1A,
278 COTL1, and PGK1 genes have been linked with “Vesicle, Cytoskeleton, Extracellular organelle,
279 Extracellular exosome, and extracellular vesicles” as shown in (Table S2: GO-CC). The
280 extracellular vesicles and associated pathways have a recognized role in osteoblast defects,
281 osteoclast development and other bone related diseases²⁸. LIMCH1 -- an actin stress fiber-
282 associated protein -- and PCH1 are downregulated in samples in this study in both the patients.
283 LIMCH1 and PHC1 both are acknowledged to have to role in skeletal muscle²⁹, and PHC1 also
284 has a function in osteoporosis, which is characterized by low bone mass and an increased risk of
285 fracture.³⁰ MRPL23 and MRPL28 are mitochondrial ribosomal proteins that are reported to play
286 a role in motor dysfunction and bone disorders^{31,32}. MYL12A has a significant function in
287 muscle accretion³³, and FGD3 is associated with bone-enlargement. TRPT1 is a downregulated
288 gene in this study and is enriched mostly with tRNA processing, splicing, via endonucleolytic
289 cleavage and ligation (GO: 0006388, 0008033). Although TRPT1 is not associated with bone
290 disease, it is highly enriched with tRNA metabolic pathways which have been reported to be
291 present in related diseases such as Paget's disease³⁴. It was also found that INTS1 is upregulated
292 in FIO patients, and upregulation in INTS1 known to have a role in the bone disposition process
293 in cell line studies³⁵. LST1 doesn't have any direct relation with bone diseases, however, it has
294 been correlated with autoimmune diseases such as rheumatoid arthritis³⁶. GNAI2 is another
295 downregulated gene in both the patients and it has been reported earlier to have role in

296 development of synovitis in osteoarthritis³⁷. EGR1 is a growth response gene that has been
297 revealed to associate with early-life loss of the bone and mechanical deformities in the bone³⁸.
298 EGR1 could be one of the genes responsible for such rapid decay and deformity. Lastly, the
299 CCDC85B gene is the part of slow-skeletal troponin I (Troponin Subunit) that is known to be a
300 protein complex that calcium binds to, thereby triggering the production of muscular force and
301 required skeleton growth^{39,40}.

302 Our study has certain limitations like small sample size, although disease is extremely rare and
303 the samples were selected from one platform. This may result in a high rate of false positive
304 results.

305 In summary, our study provides a comprehensive analysis of DEGs, biological processes terms,
306 clustering genes, and pathways, which are associated with FIO. Most of the differentially
307 expressed genes were found to be related to deficiency in bone cells and mineralization, and can
308 be used to explain the symptoms of FIO patients. These results could facilitate an improvement
309 in our comprehension of the underlying molecular mechanisms of FIO, and could stimulate
310 novel treatments for FIO. The genetic and functional analyses suggested that FIO is associated
311 with defects in osteoblast maturation, collagen fibril arrangement, matrix organization and bone
312 mineralization. The 50 gene biomarker, and their related biological process terms and pathways,
313 such as autophagy, and other signaling pathways, may represent potential targets for FIO
314 treatment and diagnosis. Additional experimental and genetic studies with a larger sample size
315 are required to confirm our results.

316

317

319 **Reference**

- 320 1. Oliver, W. C. & Pharr, G. M. An improved technique for determining hardness and
321 elastic modulus using load and displacement sensing indentation experiments. *J. Mater. Res.***7**,
322 1564–1583 (1992).
- 323 2. Das, R. *et al.* Biomechanical characterization of spider webs. *J. Mech. Behav. Biomed.*
324 *Mater.***67**, 101–109 (2017).
- 325 3. Valenti, M. T., Dalle Carbonare, L. & Mottes, M. Role of autophagy in bone and muscle
326 biology. *World J. Stem Cells***8**, 396–398 (2016).
- 327 4. Morello, R. & Esposito, P. W. Osteogenesis Imperfecta. *Osteogenes. Imperfecta* 30
- 328 5. Kimura, M. *et al.* A Critical Role for Allograft Inflammatory Factor-1 in the Pathogenesis
329 of Rheumatoid Arthritis. *J. Immunol.***178**, 3316–3322 (2007).
- 330 6. Muto, Y., Nishiyama, M., Nita, A., Moroishi, T. & Nakayama, K. I. Essential role of
331 FBXL5-mediated cellular iron homeostasis in maintenance of hematopoietic stem cells. *Nat.*
332 *Commun.***8**, 16114 (2017).
- 333 7. Ward, L. M., Hadjiyannakis, S., McMillan, H. J., Noritz, G. & Weber, D. R. Bone Health
334 and Osteoporosis Management of the Patient With Duchenne Muscular Dystrophy.
335 *Pediatrics***142**, S34–S42 (2018).
- 336 8. Cai, H. & Liu, A. Spop promotes skeletal development and homeostasis by positively
337 regulating Ihh signaling. *Proc. Natl. Acad. Sci. U. S. A.***113**, 14751–14756 (2016).
- 338 9. Tsuchie, H. *et al.* Prognosis of Primary Osteosarcoma in Elderly Patients: A Comparison
339 between Young and Elderly Patients. *Med. Princ. Pract. Int. J. Kuwait Univ. Health Sci. Cent.*
340 (2019). doi:10.1159/000500404
- 341 10. Choi, Y. J., Lee, Y. S., Lee, H. W., Shim, D. M. & Seo, S. W. Silencing of translation
342 initiation factor eIF3b promotes apoptosis in osteosarcoma cells. *Bone Jt. Res.***6**, 186–193 (2017).
- 343 11. Oh, B. *et al.* Associations of catalase gene polymorphisms with bone mineral density and
344 bone turnover markers in postmenopausal women. *J. Med. Genet.***44**, e62 (2007).
- 345 12. Shi, L. *et al.* Non-coding RNAs and LRRFIP1 Regulate TNF Expression. *J. Immunol.*
346 *Baltim. Md 1950***192**, 3057–3067 (2014).

- 347 13. Simon, A. M., Manigrasso, M. B. & O'Connor, J. P. Cyclo-oxygenase 2 function is
348 essential for bone fracture healing. *J. Bone Miner. Res. Off. J. Am. Soc. Bone Miner. Res.***17**,
349 963–976 (2002).
- 350 14. Uyama, M., Kawanami, M. & Tamura, M. Wasf2: A novel target of intermittent
351 parathyroid hormone administration. *Int. J. Mol. Med.***31**, 1243–1247 (2013).
- 352 15. SMAD-mediated modulation of YY1 activity regulates the BMP response and cardiac-
353 specific expression of a GATA4/5/6-dependent chick Nkx2.5 enhancer. - PubMed - NCBI.
354 Available at: <https://www.ncbi.nlm.nih.gov/pubmed/15329343>. (Accessed: 18th April 2019)
- 355 16. Kurth, I. *et al.* Mutations in FAM134B, encoding a newly identified Golgi protein, cause
356 severe sensory and autonomic neuropathy. *Nat. Genet.***41**, 1179–1181 (2009).
- 357 17. Carpi, D. *et al.* Dioxin-Sensitive Proteins in Differentiating Osteoblasts: Effects on Bone
358 Formation In Vitro. *Toxicol. Sci.***108**, 330–343 (2009).
- 359 18. Wirschell, M. *et al.* Building a radial spoke: flagellar radial spoke protein 3 (RSP3) is a
360 dimer. *Cell Motil. Cytoskeleton***65**, 238–248 (2008).
- 361 19. Ng, P. Y. *et al.* Disruption of the dynein-dynactin complex unveils motor-specific
362 functions in osteoclast formation and bone resorption. *J. Bone Miner. Res. Off. J. Am. Soc. Bone*
363 *Miner. Res.***28**, 119–134 (2013).
- 364 20. Ajiro, M., Jia, R., Yang, Y., Zhu, J. & Zheng, Z.-M. A genome landscape of SRSF3-
365 regulated splicing events and gene expression in human osteosarcoma U2OS cells. *Nucleic Acids*
366 *Res.***44**, 1854–1870 (2016).
- 367 21. Wang, Z., Chen, X., Zhao, Y., Jin, Y. & Zheng, J. G-protein-coupled estrogen receptor
368 suppresses the migration of osteosarcoma cells via post-translational regulation of Snail. *J.*
369 *Cancer Res. Clin. Oncol.***145**, 87–96 (2019).
- 370 22. Prahalad, S. *et al.* Variants in TNFAIP3, STAT4 and c12orf30 loci associated with
371 multiple auto-immune diseases are also associated with Juvenile Idiopathic Arthritis. *Arthritis*
372 *Rheum.***60**, 2124–2130 (2009).
- 373 23. Ma, F., Zhang, C., Prasad, K. V., Freeman, G. J. & Schlossman, S. F. Molecular cloning
374 of Porimin, a novel cell surface receptor mediating oncotic cell death. *Proc. Natl. Acad. Sci. U.*
375 *S. A.***98**, 9778–9783 (2001).
- 376 24. Zhang, C., Xu, Y., Gu, J. & Schlossman, S. F. A cell surface receptor defined by a mAb
377 mediates a unique type of cell death similar to oncosis. *Proc. Natl. Acad. Sci. U. S. A.***95**, 6290–
378 6295 (1998).

- 379 25. Eswarakumar, V. P. *et al.* The IIIc alternative of Fgfr2 is a positive regulator of bone
380 formation. *Dev. Camb. Engl.***129**, 3783–3793 (2002).
- 381 26. Bredella, M. A. *et al.* Ectopic and Serum Lipid Levels Are Positively Associated with
382 Bone Marrow Fat in Obesity. *Radiology***269**, 534–541 (2013).
- 383 27. Jafarifar, F., Dietrich, R. C., Hiznay, J. M. & Padgett, R. A. Biochemical defects in minor
384 spliceosome function in the developmental disorder MOPD I. *RNA***20**, 1078–1089 (2014).
- 385 28. Liu, M., Sun, Y. & Zhang, Q. Emerging Role of Extracellular Vesicles in Bone
386 Remodeling. *J. Dent. Res.***97**, 859–868 (2018).
- 387 29. Kassianidou, E. & Kumar, S. A biomechanical perspective on stress fiber structure and
388 function. *Biochim. Biophys. Acta***1853**, 3065–3074 (2015).
- 389 30. Karasik, D., Rivadeneira, F. & Johnson, M. L. The genetics of bone mass and
390 susceptibility to bone diseases. *Nat. Rev. Rheumatol.***12**, 323–334 (2016).
- 391 31. Wang, W. *et al.* Ribosomal Proteins and Human Diseases: Pathogenesis, Molecular
392 Mechanisms, and Therapeutic Implications. *Med. Res. Rev.***35**, 225–285 (2015).
- 393 32. Serre, V. *et al.* Mutations in mitochondrial ribosomal protein MRPL12 leads to growth
394 retardation, neurological deterioration and mitochondrial translation deficiency. *Biochim.*
395 *Biophys. Acta***1832**, 1304–1312 (2013).
- 396 33. Pérez O’Brien, A. M. *et al.* Assessing signatures of selection through variation in linkage
397 disequilibrium between taurine and indicine cattle. *Genet. Sel. Evol. GSE***46**, 19 (2014).
- 398 34. Piccirilli, J. A. & Koldobskaya, Y. Crystal structure of an RNA polymerase ribozyme in
399 complex with an antibody fragment. *Philos. Trans. R. Soc. B Biol. Sci.***366**, 2918–2928 (2011).
- 400 35. Caputo, M. *et al.* Effect of low frequency (LF) electric fields on gene expression of a
401 bone human cell line. *Electromagn. Biol. Med.***33**, 289–295 (2014).
- 402 36. Liu, G. *et al.* Cis-eQTLs regulate reduced LST1 gene and NCR3 gene expression and
403 contribute to increased autoimmune disease risk. *Proc. Natl. Acad. Sci.***113**, E6321–E6322
404 (2016).
- 405 37. Huang, H. *et al.* Identification of pathways and genes associated with synovitis in
406 osteoarthritis using bioinformatics analyses. *Sci. Rep.***8**, (2018).
- 407 38. Reumann, M. K. *et al.* Early growth response gene 1 regulates bone properties in mice.
408 *Calcif. Tissue Int.***89**, 1–9 (2011).
- 409 39. Johnston, J. R., Chase, P. B. & Pinto, J. R. Troponin through the looking-glass: emerging
410 roles beyond regulation of striated muscle contraction. *Oncotarget***9**, 1461–1482 (2017).

- 411 40. Ju, Y. *et al.* Troponin T3 expression in skeletal and smooth muscle is required for growth
412 and postnatal survival: Characterization of Tnnt3tm2a(KOMP)Wtsi mice. *Genes. N. Y. N*
413 *2000***51**, 667–675 (2013).
- 414 41. Ralphs JR , Stamp TC , Dopping-Hepenstal PJ , Ali SY . Ultrastructural features of the
415 osteoid of patients with fibrogenesis imperfecta ossium. *Bone* . 1989;10(4):243–249.
- 416 42. Carr AJ , Smith R , Athanasou N , Woods CG . Fibrogenesis imperfecta ossium. *J Bone*
417 *Joint Surg Br* . 1995;77(5):820–829.
- 418 43. Bhadada, Sanjay Kumar et al. “Fibrogenesis Imperfecta Ossium and Response to Human
419 Growth Hormone: A Potential Therapy.” *The Journal of clinical endocrinology and*
420 *metabolism* 102 5 (2017): 1750-1756 .
- 421 44. Bhadada SK, Dhaliwal R, Dhiman V, Rao SD. Fibrogenesis Imperfecta Ossium. *Calcif*
422 *Tissue Int.* 2019;104:561-569.
- 423 45. Dhaliwal R, Dhiman V, Rao DS, Bhadada SK. Fibrogenesis Imperfecta Ossium: Clinical
424 Approach to Diagnosis and Management of a Rare Skeletal Disorder. *The Journal of Clinical*
425 *Endocrinology & Metabolism.*2019;104:4005-40015.

426 **Figure Legends**

427 Figure 1. Chart showing the workflow used to do bioinformatics analysis

428 Figure 2. Shown PCA (Principal Component Analysis) was performed on GSE43861 to reduce
429 dimensionality and bring out patterns in the dataset.

430 Figure 3 Co-expression network interaction. Figure 3a Showing clustering method and Figure 3b
431 Showing the analysis of iActiveModules based on expression levels. Figure 3c. Clustering
432 showing the cluster with maximum connectivity

433 Figure 4 Heat map showing the expression of the 50 genes that were selected based on the
434 clustering analysis and compares the control samples with the two FIO patient samples.

435

436 Figure 5 Pathways/Area of effect associated with FIO Figure 5a show an Ingenuity Pathway
437 Analysis (IPA) network diagram. Figure 5b shows a heatmap of the 50 selected genes with their
438 associated pathways/areas of effect.

439

440

Figures

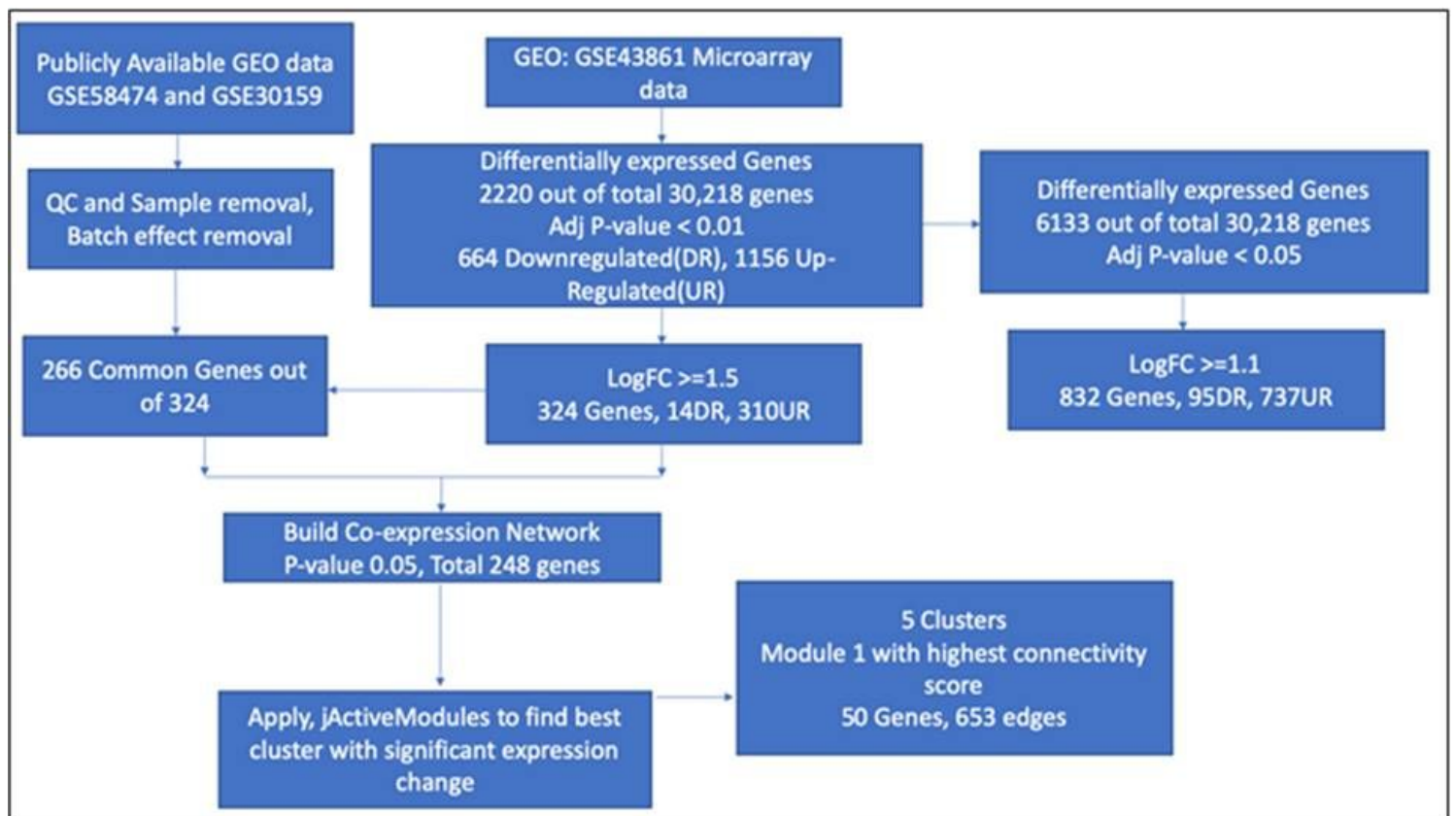


Figure 1

Chart showing the workflow used to do bioinformatics analysis

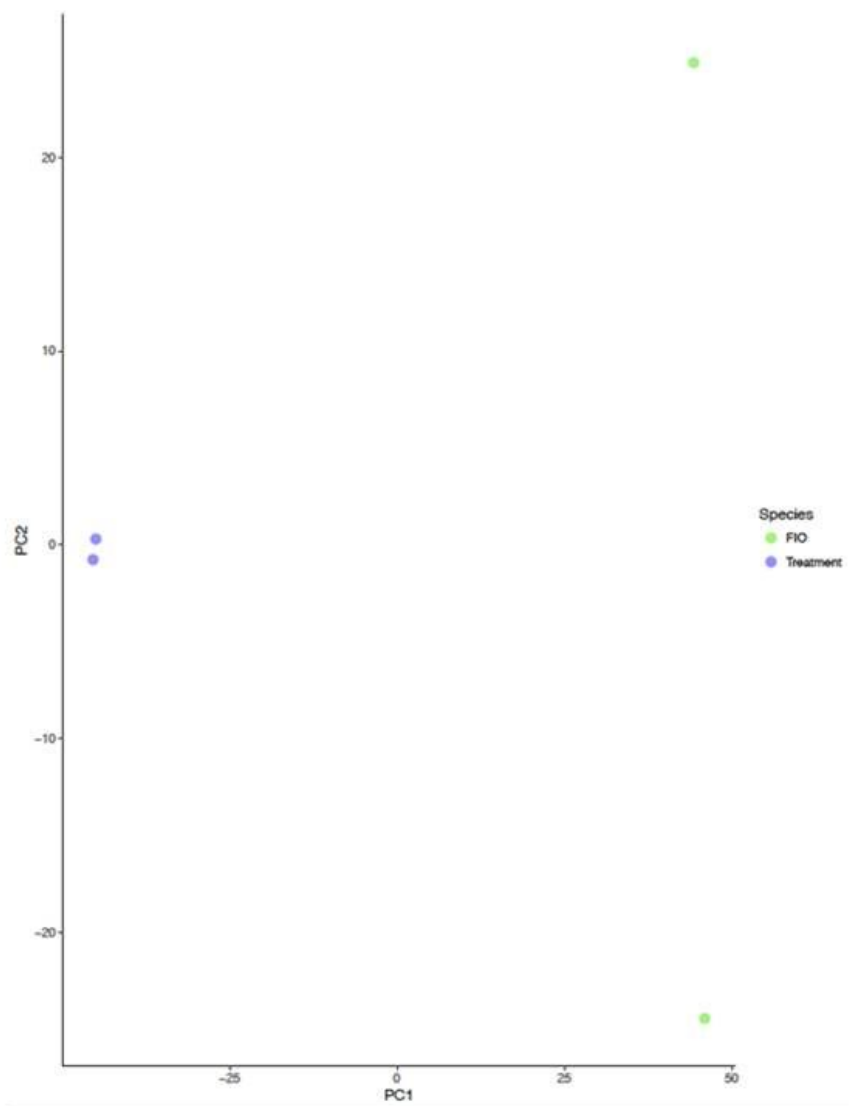


Figure 2

Shown PCA (Principal Component Analysis) was performed on GSE43861 to reduce dimensionality and bring out patterns in the dataset.

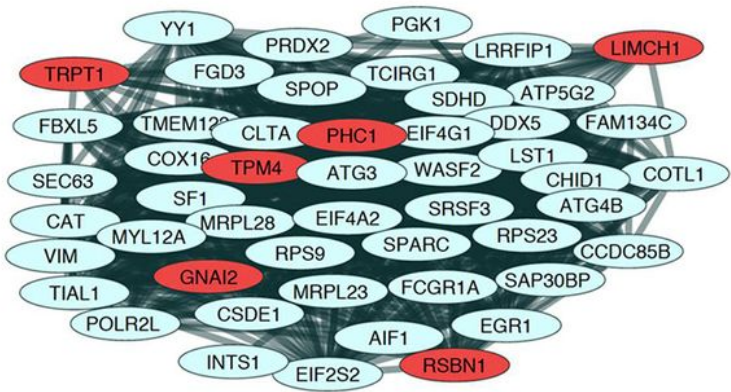
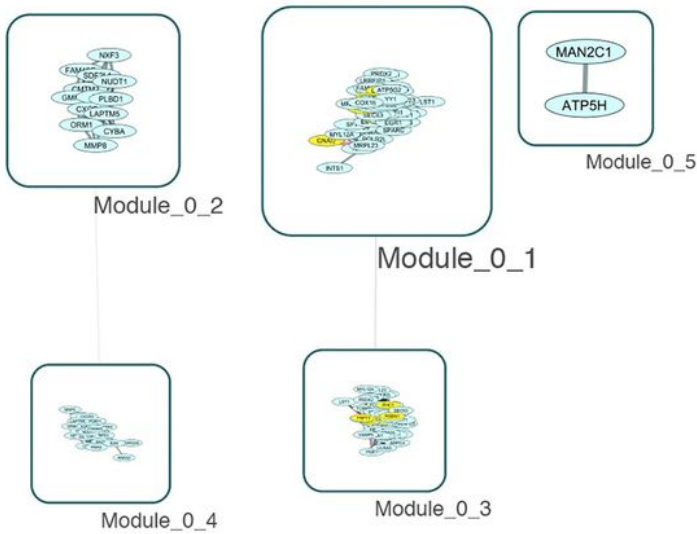
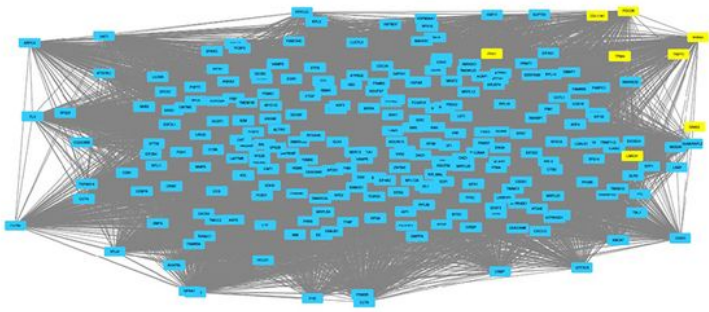


Figure 3

Co-expression network interaction. Figure 3a Showing clustering method and Figure 3b Showing the analysis of iActiveModules based on expression levels. Figure 3c. Clustering showing the cluster with maximum connectivity

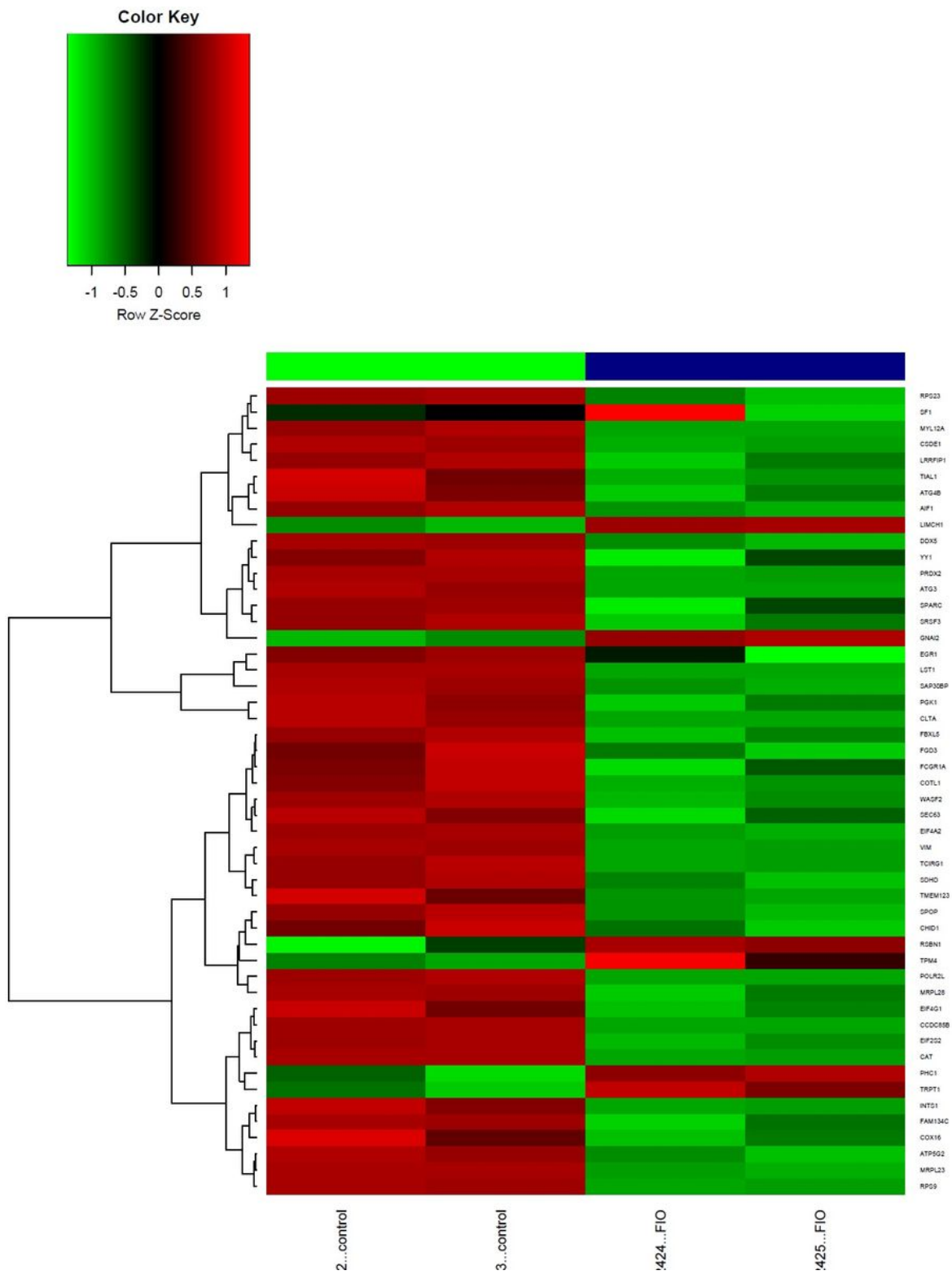


Figure 4

Heat map showing the expression of the 50 genes that were selected based on the clustering analysis and compares the control samples with the two FIO patient samples.

This is a list of supplementary files associated with this preprint. Click to download.

- [TableS1.txt](#)
- [TableS2.xlsx](#)
- [FigureS3C.jpg](#)
- [FigureS3C.jpg](#)
- [Table4.jpg](#)